

Catalyst-free GaN Nanowire Growth and Optoelectronic Characterization*

Kris A. Bertness^a, Norman A. Sanford, John B. Schlager
National Institute of Standards and Technology, 325 Broadway, Boulder, CO, USA 80305-3328;

ABSTRACT

We discuss the present state-of-the-art concerning the growth mechanism, optical luminescence and electrical properties for GaN nanowires grown with catalyst-free molecular beam epitaxy. These nanowires are essentially defect-free and display long photoluminescence lifetimes and carrier mobilities relative to epitaxially grown GaN films. The exclusion of crystalline defects comes from the ease with which strain-relieving dislocations can reach the sidewalls and terminate. The growth mechanism is based on variations in Ga sticking coefficients and surface energies of the sidewall planes and end facet planes. With control of the nucleation process through selective epitaxy on patterned substrates, a high degree of diameter, length and position control can be achieved. Common difficulties with interpretation of optical and electrical data with regard to internal quantum efficiency and mobility are also addressed.

Keywords: GaN nanowires, molecular beam epitaxy, photoluminescence, growth mechanism

1. INTRODUCTION

Because of the unique mechanism by which catalyst-free GaN nanowires grow during molecular beam epitaxy (MBE), they are among the purest forms of GaN readily achievable, being free of crystalline defects and low in chemical impurities. This condition is achieved with a combination of high purity source materials and growth environment and a nucleation mode that excludes lattice mismatch defects to the free surfaces within 10 nm of growth. The continued proximity of the free surface also permits the addition of strained heterojunctions without defect formation. This paper will discuss the structural, optical and electrical properties of these nanowires to support these assertions.

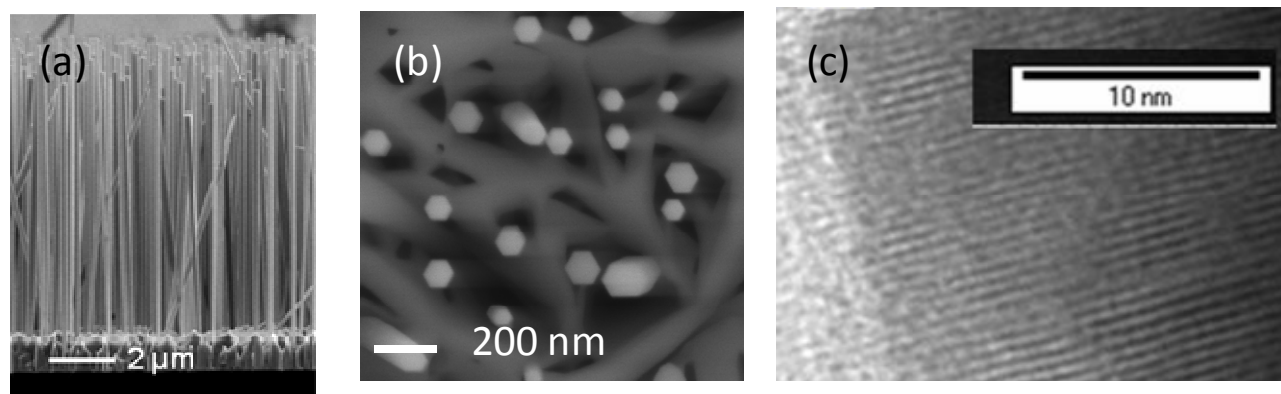


Figure 1. Morphology of GaN nanowires shown in (a) cross-sectional (SEM), (b) plan view SEM, and (c) high resolution lattice images generated with TEM. The latter show that the material is free of dislocations.

*Contribution of an agency of the U.S. government; not subject to copyright.

^abertness@boulder.nist.gov; phone 1 303 497-5069; fax 1 303 497-3387

The morphology of well-separated GaN nanowires is illustrated with scanning electron microscopy (SEM) in Fig. 1(a) and (b). The nanowires grow along the $[0\ 0\ 0\ 1]$ crystal direction (c -axis of the wurtzite crystal structure) with sidewalls that conform to the $\{1\bar{1}0\ 0\}$ family of m -planes.¹⁻³ The cross-sections are six-sided, and often form nearly perfect hexagons as shown in Fig. 1(b). As discussed further below, the growth mechanism prevents the propagation of threading dislocations in the nanowires, producing defect-free material, as shown in the high resolution lattice image made by transmission electron microscopy (TEM) in Fig. 1(c). Diameters vary from 30 nm to 900 nm, with most falling between 150 nm to 300 nm. Length is controlled primarily by growth time, though coalescence of dense nanowires can prevent the achievement of the $> 10\ \mu\text{m}$ lengths seen in Fig. 1(a).

2. CRYSTAL GROWTH MECHANISM

2.1 MBE Conditions

GaN nanowires nucleate spontaneously at high substrate temperature (780 °C to 830 °C) and high N_2 overpressure relative to the Ga flux.^{4,5} As with any growth of GaN via MBE, the N_2 reaction rate is insufficient unless the N_2 is passed through a plasma, typically maintained with radio frequency (RF) radiation, though electron cyclotron resonance has also been used. Because of the variety of aperture and plasma confinement designs, there is considerable variation in the actual species produced by these N_2 sources, and this variability is likely to be a major source of differences in the exact growth conditions from laboratory to laboratory. The Ga beam equivalent pressure is typically around 2×10^{-5} Pa, leading to growth rates about $200\ \text{nm h}^{-1}$.

The most widely used substrate is Si(111) with a final cleaning step of HF acid (1:10 HF:H₂O for 120 s in our laboratory) to remove native oxides. The substrates are heated in vacuum to high temperature ($\sim 850\ ^\circ\text{C}$) prior to growth. Some workers heat until the Si(111) (7×7) reconstruction appears.⁶ Nanowires grown on Si(111) are well-aligned azimuthally to the underlying Si planes, allowing x-ray diffraction studies of ensembles of nanowires. Nanowire growth has also been demonstrated on Si(100) and on sapphire substrates,^{7,8} but the alignment with the substrate is weaker and the cross-sections, while still six-sided, diverge greatly from the equilateral edges that give the “perfect” hexagon shape in Fig. 1(b). AlN buffer layers are frequently used to increase the uniformity of nucleation, and these layers have a profound effect on the nucleation process.^{9,10}

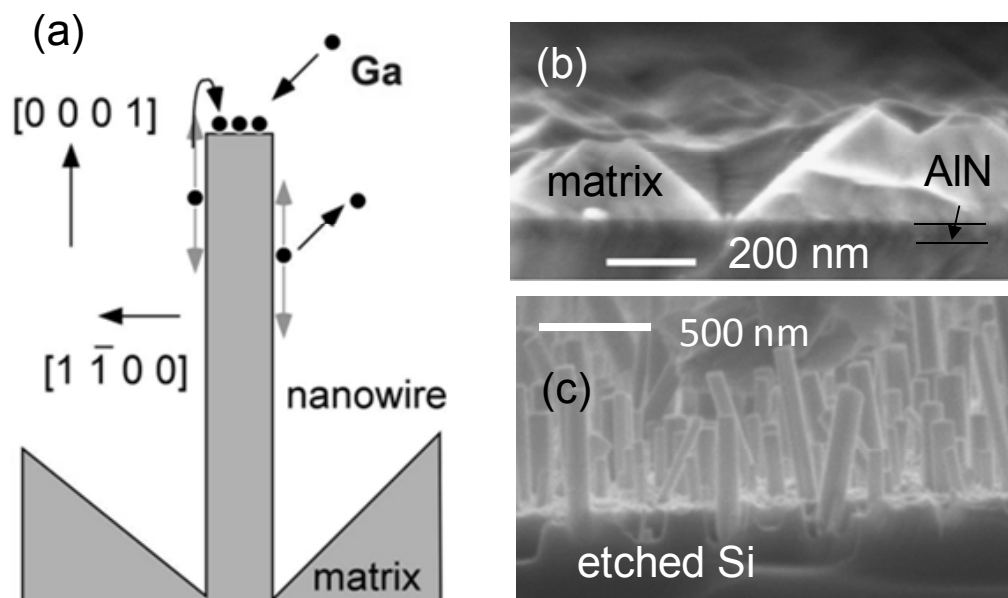


Figure 2. (a) Schematic illustration of growth mechanism for GaN nanowires in MBE. (b) and (c) illustrate enhancement of nucleation in pitted regions formed spontaneously in GaN (b) and by etching Si (c).

2.2 Growth Mechanism

The mechanism for the growth of GaN nanowires in MBE is most simply understood by separating growth into two stages — nucleation and propagation. The propagation mechanism, illustrated in Fig. 2, is based on the differences in sticking coefficient for Ga on the different crystal planes.^{8, 9, 11} These sticking coefficient variations in turn are correlated with the minimization of total surface energy in the crystal,¹² and are likely to play a role in the initial seed crystal formation as well. The sticking coefficient on the end plane, a *c*-plane, is significantly higher than on the *m*-plane sidewalls. Ga atoms that impinge directly on the tip are incorporated into the growing crystal, but Ga atoms that strike the *m*-plane sidewalls will either diffuse to the end of the wire and incorporate there (left side in Fig. 2), or they desorb back into vacuum (right side in Fig. 2). Nanowires rarely terminate with facets other than a flat *c*-plane, but the rare observations of tilted tips do suggest that intermediate sticking coefficient ratios exist for such planes. As will be discussed further below, tilted end facets are the rule rather than the exception in selective epitaxy of GaN nanowires.

This propagation mode is distinctly different from the vapor-liquid-solid (VLS) mode used to grow nanowires in a variety of materials systems by use of metal catalysts. Early in the history of research on GaN nanowires, many hypothesized that the growth might proceed through nanoscale Ga droplet formation and subsequent VLS growth. As illustrated in Table 1, there are a number of significant differences in the observations of growth morphology and structure between these methods. The absence of even a single observation of a surviving Ga droplet also argued against the self-catalysis hypothesis, and more extreme experiments confirmed that the droplets were not present even under conditions favorable to their formation and survival.⁸ Intentionally created Ga droplets were also found to have no effect on nanowire growth other than to serve as small reservoirs of Ga atoms.¹³ Under some conditions, thicker nanowires grow more slowly in length than thinner ones, which has been attributed to conditions in which the Ga diffusion length on the sidewalls is larger than the diameter of the wire.^{14, 15} Other workers have found slight *increases* in growth rate as diameter increases, and attribute the variation to chemical potential and surface energy driving forces.³ Clearly as the density and length increase, shadowing of the molecular beam and recycling of Ga desorbing from sidewalls⁸ can also become significant factors in the relative growth rates on sidewalls and end tips.

Early in the formation of GaN nanowires, the strain mismatch is accommodated with dislocations and stacking faults that glide to the edge of the nanowire and terminate.^{16, 17} This exclusion mechanism does not operate for *a*-axis nanowires grown with other methods, for which stacking faults and twin boundaries propagate indefinitely along the growth axis.¹⁸

Table 1. Comparison of crystal properties for GaN nanowires grown with catalyst particles and via spontaneous nucleation. The large differences are one indication that spontaneous nanowire growth is *not* caused by self-catalysis.

Property / Growth Method	Catalytic	Spontaneous
Orientation	Typically <i>a</i> -axis, some <i>m</i> -axis, <i>c</i> -axis	<i>c</i> -axis only, with <i>m</i> -plane sidewalls
Cross-section	Rough, circular, triangular, belts, etc	Smooth facets, six-sided
Length uniformity	Poor, varies with nucleation time	Length uniform within 5 %
Diameter uniformity	Determined by catalyst particle size	Varies dramatically; diameter and hexagonal uniformity depend on nucleation details
Growth rate	10 – 100 $\mu\text{m/h}$	< 0.1 – 0.3 $\mu\text{m/h}$
V:III ratio	Not critical	High V:III ratio essential
Growth temperature	Not critical	Temperature high, near equilibrium with Ga vapor, narrow range (~ 30 °C)

While the differential sticking coefficient propagation mechanism appears to apply to most nanowire growth conditions and explains the ubiquity of c -axis orientation and six-sided cross-section, the nucleation process is quite sensitive to initial conditions and leads to much variation in the size, shape, and density of the nanowires from laboratory to laboratory and run to run. Nucleation within a regularly faceted pit, such as one formed by $\{1\bar{1}02\}$ planes shown in Fig. 2, leads to well-separated nanowires with mostly even sidewall lengths. These pits form on smooth AlN buffer layers.⁹ Nucleation on Si(100),^{7,9} at a high growth temperature and Ga flux¹³ or on bare Si,¹⁵ on the other hand, seem to inhibit matrix layer formation. The nanowires nucleated under these conditions are less symmetric in cross-section and tend toward higher density, which leads to early coalescence. As shown in Fig. 2 (c), nanowire nucleation can also be enhanced with the formation of pits.

2.3 Selective Epitaxy

The preceding arguments suggest that with careful control of the nucleation process, nanowire dimensions can be controlled to high precision. Patterned epitaxy is difficult in MBE, but two groups have shown that good results can be obtained with Ti metal masks that are nitrided *in situ*¹⁹ and with SiN_x masks on AlN buffer layers.²⁰ The diameter control available with TiN_x masks has been used to control In incorporation in InGaN quantum disks grown into the nanowires, in turn producing photoluminescence that is highly uniform in color.²¹ An example of the morphology that can be obtained with SiN_x masks is given in Fig. 3. Arrays such as those shown in Fig. 3(a) vary by less than 5 % in diameter, and essentially perfect selectivity (defined as grown within the mask openings but no growth outside openings) has been obtained over 95 % of the usable wafer area. Fig. 2(a) also illustrates how the mask area is completely free of GaN deposition, unlike with the TiN_x approach. The nanowires at the mask edge are similar in growth rate to those in the center of the array, which indicates that the mask serves as neither a source nor a sink of Ga atoms, i. e., that diffusion of Ga atoms on the mask is negligible. For both masking methods, the growth parameter range for selective growth is narrower than for random nanowire nucleation; specifically, higher substrate temperature and lower Ga flux are typically required to suppress nucleation on the mask.

In both of these studies as well as in patterned epitaxy with organometallics vapor phase epitaxy,²² the tips of the nanowires take on a distinct faceted shape conforming to $\{1\bar{1}0n\}$ planes where $n = 2$ or 3, provided the diameter is smaller than around 500 nm. Recent studies of the nucleation process identified several distinct stages including the formation of pyramids with $\{1\bar{1}03\}$ facets, which also appear in quantum dot growth of GaN on AlN.²³ These observations again support the growth model that nanowire growth is driven largely by thermodynamic effects such as surface energy variations over different crystallographic planes, and that the nanowires tend to maintain the shape of the original seed crystal even during the propagation phase.

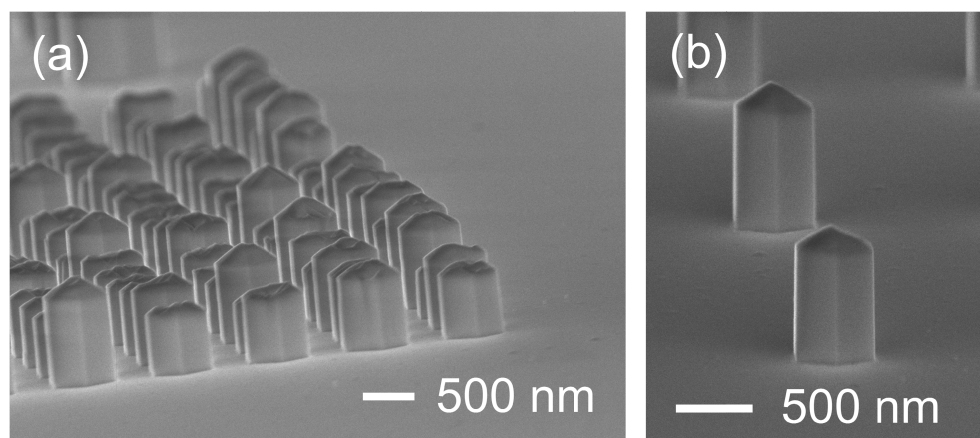


Figure 3. GaN nanowires grown with selective epitaxy on SiN_x masks. Nanowires grow only in openings etched through the SiN_x to the underlying AlN buffer layer.

3. OPTICAL AND ELECTRICAL PROPERTIES

3.1 Photoluminescence (PL)

GaN nanowires grown with MBE have high optical emission intensities, such that luminescence from single nanowires is readily observed with HeCd laser excitation (325 nm, 3.815 eV).^{24, 25} Several groups have reported that the dominant low-temperature PL peak occurs at the unstrained energy position for the donor-bound exciton D^0X_A peak of 3.472 eV.^{2, 3, 6, 25, 26} Yellow luminescence and other defect-related luminescence are absent unless nanowire coalescence has occurred or the specimen includes the matrix layer. Time-resolved PL indicates that the minority carrier lifetime at room temperature is limited by surface recombination, and that the surface recombination velocity is quite low at $9 \times 10^3 \text{ cm s}^{-1}$ (see Fig. 4).²⁴ Even with this limitation, the PL lifetime is longer in MBE-grown GaN nanowires than in most epitaxial GaN films, including those grown on nonpolar substrates.²⁷

Temperature-dependent measurements of PL lifetime reveal that the dominant recombination processes change with temperature, from bound-exciton recombination to free-exciton recombination to surface recombination, and that the relative influence of these processes is strongly dependent on excitation intensity.^{24, 28} Although it is tempting to apply simplistic models for internal quantum efficiency such as taking the ratio of PL intensity at room temperature to that at low temperature, this ratio is likely to be meaningless for a single PL measurement and in fact does not work well for nitrides in general.²⁹ Thermal drift of the beam relative to the nanowire and intensity variations common in ultraviolet laser sources add to the uncertainty. With identification of the temperature range and excitation levels at which radiative recombination mediated by free excitons determines the PL lifetime, the internal quantum efficiency of MBE-grown GaN nanowires at room temperature has been estimated to be $\sim 30\%$.²⁸

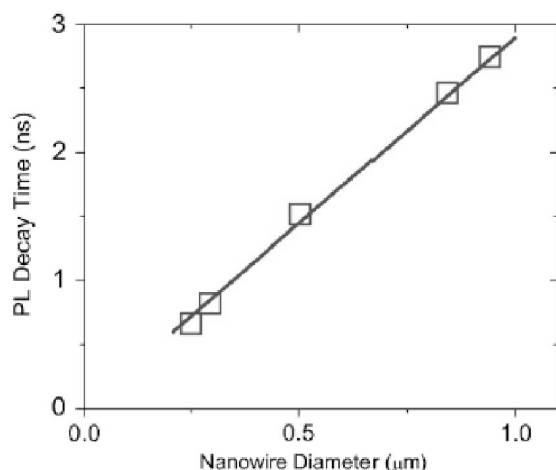


Figure 4. PL decay time at room temperature as a function of nanowire diameter for a set of GaN nanowires from the same growth run. The linear dependence of decay time on diameter indicates that surface recombination is the dominant decay mechanism, and the slope of the line yields a surface recombination velocity of $9 \times 10^3 \text{ cm s}^{-1}$.

3.2 Electrical properties

Carrier concentration measurements in semiconductor nanowires are quite difficult because methods developed for epitaxial thin films, such as Hall mobility and capacitance-voltage measurements, are beyond the state-of-the-art for contact fabrication and standard instrumentation sensitivity. The ability to grow nanowires sufficiently long to readily disperse them onto insulating substrates and contact the ends with conventional photolithography has been critical to obtaining reliable information about the carrier concentration and mobility. We have found that modeling resistance as a function of nanowire length, radius, and contact area for sets of ten or more n-type (Si-doped) GaN nanowires from the same growth run gives carrier concentration and mobility results with moderate uncertainty.³⁰ Key assumptions in this analysis are that the dopant concentration and surface potential are uniform across the sample set, the contact resistivity is known, and the surface potential can be assumed to fall within a range of a few electron volts.

Transient photoconductivity measurements^{31, 32} provide valuable insight for narrowing the range of surface potential values, particularly for nanowires that are fully depleted in the dark. For the latter, the surface band bending in the dark, Φ_m , is determined by the maximum number of carriers available from the bulk dopant atoms to fill the surface states, rather than the poorly known surface state densities, energy level(s), and capture cross-sections. Φ_m can be derived from the photoconductivity decay time τ near the restoration of the dark condition, and can be related to the carrier concentration as $\Phi_m = q N_d R_m^2 / 4\epsilon$, where q is the electronic charge, N_d is the donor atomic concentration, R_m is the nanowire radius, and ϵ is the dielectric constant of the nanowire. (See Ref. 31 for a discussion of the appropriate approximation for R_m in these hexagonal cross-section wires.) Because $\tau = \tau_c \exp(\Phi_m / kT)$, the slope of $\ln(\tau / \tau_c)$ vs R^2 is equal to $q N_d / 4 \epsilon$, where τ_c is the capture time for the electrons entering the charged surface state in the absence of a surface band bending barrier, k is the Boltzmann constant, and T is the absolute temperature. Because only the slope is needed, τ_c can be chosen arbitrarily for plotting convenience. (Conversely, this implies data on Φ_m for depleted nanowires cannot be used to determine the capture cross-section of the surface states that produce the band-bending.) An example is given in Fig. 5 for nanowires from a long undoped run (B992 from Ref. 31). More information including treatment of nanowires that are conductive in the dark can be obtained from time-dependent fits of the photoconductivity decay.³¹

These methods indicate that for MBE-grown GaN nanowires, the mobility as a function of carrier concentration varies from $500 \text{ cm}^2 \text{ V}^{-1} \text{ s}^{-1}$ ($N_d = 3 \times 10^{16} \text{ cm}^{-3}$) to $700 \text{ cm}^2 \text{ V}^{-1} \text{ s}^{-1}$ ($N_d = 1 \times 10^{16} \text{ cm}^{-3}$) for n -type nanowires with low residual doping, and from $300 \text{ cm}^2 \text{ V}^{-1} \text{ s}^{-1}$ ($N_d = 1 \times 10^{18} \text{ cm}^{-3}$) to $600 \text{ cm}^2 \text{ V}^{-1} \text{ s}^{-1}$ at ($N_d = 6 \times 10^{17} \text{ cm}^{-3}$) for intentionally doped nanowires. These mobility values are somewhat higher than for typical epitaxial material, but do not exceed the best values reported for such films.³³ The mobility is also *independent* of diameter for the range explored ($> 70 \text{ nm}$).

Early work explored the use of field effect transistor (FET) transconductance and threshold voltage measurements to separate mobility from carrier concentration. Because of the extreme difficulty in fabricating gate contacts on nanowires and in measuring contact or gate capacitance, typical sample geometry consisted of a nanowire dispersed onto an oxidized Si substrate with source and drain contacts fabricated at the two nanowire ends. The Si substrate itself was biased to form a “back-gate,” and the capacitance between the nanowire and the substrate was modeled as an ideal conducting wire embedded in a dielectric material far above a conducting plane. There are a number of systematic errors introduced by this approach,^{34, 35} and we have also observed hysteresis with light exposure and bias^{30, 36} that point to influence by trapped charge in the nearby dielectrics (typically SiO_x). The systematic modeling errors have a dependence on nanowire diameter that can erroneously confer diameter dependence to the mobility determination where none actually exists. Although back-gated measurements can perhaps provide an estimate on carrier concentration to within one or two orders of magnitude, they cannot be relied on for accurate determination of absolute values or for relative measurements when the geometry of nanowires or dielectric varies.

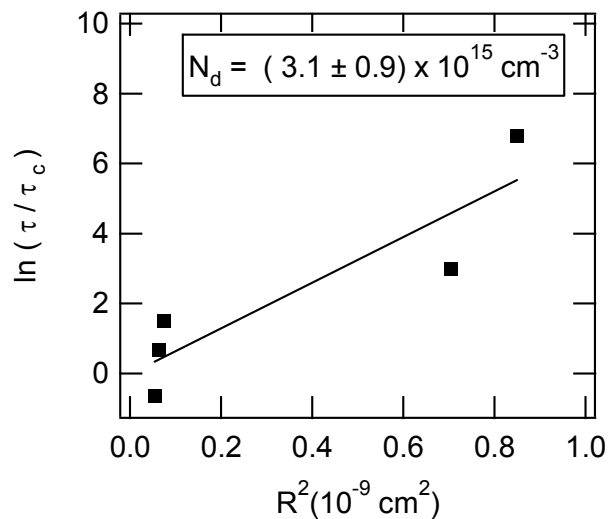


Figure 5. Graphical solution of photoconductivity decay time data vs. the square of nanowire radius to extract carrier concentration. This method applies only to nanowires that are fully depleted of free carriers in the dark.

A major unsolved difficulty for MBE-grown GaN nanowires is the clear demonstration and characterization of *p*-type doping. This difficulty is not surprising given that *p*-type doping in films has only been demonstrated with one dopant species, Mg, for which the electrical activation is so poor that practical application was not possible until the 1990s. Although bright nanowire light-emitting diodes have been made from MBE-grown GaN nanowires,³⁷ the *p*-type region of these devices were grown with lower substrate temperatures such that the diameter increased rapidly with length and a coalesced top surface was produced. In our laboratory we have observed indications of low free hole concentration and Mg incorporation in electroluminescence, PL, SIMS and SEM contrast. Data demonstrating a linear dependence of current vs. voltage (i. e., ohmic behavior) through a single *p*-type GaN nanowire, however, have yet to be published by any group working in this field. This step is a precursor to actual free hole concentration measurement. Our current hypothesis is that the difficulties come from a combination of incorporating sufficient Mg at the high growth temperatures required for nanowire growth and the three-dimensional nature of a nanowire contact.

4. SUMMARY

Catalyst-free growth of GaN nanowires is shown to produce material of exceptional quality, often exceeding what can be obtained in thin films and bulk crystals. The unique growth mechanism allows lattice mismatch strain with growth substrates to be relieved within a few nanometers of nucleated growth, and these defects terminate at the nanowire walls. Unlike growth via the VLS mechanism, catalyst-free GaN nanowire growth derives from variations in surface energies and sticking coefficients among the wurtzite crystal planes. Excellent control of diameter, length and position are possible with selective epitaxy based on patterned masks of TiN_x and SiN_x. MBE-grown GaN nanowires are defect free with low background carrier concentration, enabling doping with the intentional addition of Si for *n*-type and Mg for *p*-type. Measurements of *n*-type free carrier concentration show excellent mobility; work on *p*-type material has been limited due to the inability to establish ohmic contacts with what may be only lightly doped material. The optical properties show that the nanowires should make efficient luminescence sources, having long minority carrier lifetime and low surface recombination velocity. The surface recombination velocity limits optical efficiency at room temperature. The major challenges ahead for this technology include demonstration of free hole concentration measurement and electrical contact formation.

REFERENCES

- [1] Bertness, K. A., Schlager, J. B., Sanford, N. A., Roshko, A., Harvey, T. E., Davydov, A. V., Levin, I., Vaudin, M. D., Barker, J. M., Blanchard, P. T. and Robins, L. H., "High degree of crystalline perfection in spontaneously grown GaN nanowires," Mater. Res. Soc. Symp. Proc. 892, Warrendale, PA, 0892-FF0831-0803 (2005).
- [2] Chen, H. Y., Lin, H. W., Shen, C. H. and Gwo, S., "Structure and photoluminescence properties of epitaxially oriented GaN nanorods grown on Si(111) by plasma-assisted molecular-beam epitaxy," Appl. Phys. Lett. 89, 243105 (2006).
- [3] Tchernycheva, M., Sartel, C., Cirlin, G., Travers, L., Patriarche, G., Harmand, J. C., Dang, L. S., Renard, J., Gayral, B., Nevou, L. and Julien, F., "Growth of GaN free-standing nanowires by plasma-assisted molecular beam epitaxy: structural and optical characterization," Nanotechnology 18, 385306 (2007).
- [4] Yoshizawa, M., Kikuchi, A., Mori, M., Fujita, N. and Kishino, K., "Growth of self-organized GaN nanostructures on Al₂O₃(0001) by RF-radical source molecular beam epitaxy," Jpn. J. Appl. Phys. Part 2 36, L459-L462 (1997).
- [5] Sánchez-García, M. A., Calleja, E., Monroy, E., Sanchez, F. J., Calle, F., Munoz, E. and Beresford, R., "The effect of the III/V ratio and substrate temperature on the morphology and properties of GaN- and AlN-layers grown by molecular beam epitaxy on Si(111)," J. Cryst. Growth 183, 23-30 (1998).
- [6] Songmuang, R., Landre, O. and Daudin, B., "From nucleation to growth of catalyst-free GaN nanowires on thin AlN buffer layer," Appl. Phys. Lett. 91, 251902 (2007).
- [7] Cerutti, L., Ristić, J., Fernandez-Garrido, S., Calleja, E., Trampert, A., Ploog, K. H., Lazic, S. and Calleja, J. M., "Wurtzite GaN nanocolumns grown on Si(001) by molecular beam epitaxy," Appl. Phys. Lett. 88, 213114 (2006).

- [8] Bertness, K. A., Roshko, A., Mansfield, L. M., Harvey, T. E. and Sanford, N. A., "Mechanism for spontaneous growth of GaN nanowires with molecular beam epitaxy," *J. Cryst. Growth* 310, 3154-3158 (2008).
- [9] Bertness, K. A., Roshko, A., Mansfield, L. M., Harvey, T. E. and Sanford, N. A., "Nucleation conditions for catalyst-free GaN nanowires," *J. Cryst. Growth* 300, 94-99 (2007).
- [10] Ristić, J., Sánchez-García, M. A., Calleja, E., Sanchez-Paramo, J., Calleja, J. M., Jahn, U. and Ploog, K. H., "AlGa_N nanocolumns grown by molecular beam epitaxy: Optical and structural characterization," *Phys. Status Solidi A-Appl. Res.* 192, 60-66 (2002).
- [11] Bertness, K. A., Sanford, N. A., Barker, J. M., Schlager, J. B., Roshko, A., Davydov, A. V. and Levin, I., "Catalyst-free growth of GaN nanowires," *J. Electron. Mat.* 35, 576-580 (2006).
- [12] Lymperakis, L. and Neugebauer, J., "Large anisotropic adatom kinetics on nonpolar GaN surfaces: Consequences for surface morphologies and nanowire growth," *Phys. Rev. B* 79, 241308 (2009).
- [13] Ristic, J., Calleja, E., Fernandez-Garrido, S., Cerutti, L., Trampert, A., Jahn, U. and Ploog, K. H., "On the mechanisms of spontaneous growth of III-nitride nanocolumns by plasma-assisted molecular beam epitaxy," *J. Cryst. Growth* 310, 4035-4045 (2008).
- [14] Debnath, R. K., Meijers, R., Richter, T., Stoica, T., Calarco, R. and Luth, H., "Mechanism of molecular beam epitaxy growth of GaN nanowires on Si(111)," *Appl. Phys. Lett.* 90, 123117 (2007).
- [15] Calarco, R., Meijers, R. J., Debnath, R. K., Stoica, T., Sutter, E. and Luth, H., "Nucleation and growth of GaN nanowires on Si(111) performed by molecular beam epitaxy," *Nano Lett.* 7, 2248-2251 (2007).
- [16] Trampert, A., Ristic, J., Jahn, U., Calleja, E. and Ploog, K. H., "TEM study of (Ga,Al)_N nanocolumns and embedded GaN nanodiscs," in *Microscopy Of Semiconducting Materials 2003*, IOP Publishing Ltd, Bristol, 167-170 (2003).
- [17] Calleja, E., Ristic, J., Fernandez-Garrido, S., Ceruffi, L., Sanchez-Garcia, M. A., Grandal, J., Trampert, A., Jahn, U., Sanchez, G., Griol, A. and Sanchez, B., "Growth, morphology, and structural properties of group-III-nitride nanocolumns and nanodisks," *Physica Status Solidi B-Basic Solid State Physics* 244, 2816-2837 (2007).
- [18] Tham, D., Nam, C.-Y. and Fischer, J. E., "Defects in GaN Nanowires," *Advanced Functional Materials* 16, 1197-1202 (2006).
- [19] Kishino, K., Sekiguchia, H. and Kikuchi, A., "Improved Ti-mask selective-area growth (SAG) by rf-plasma-assisted molecular beam epitaxy demonstrating extremely uniform GaN nanocolumn arrays," *J. Cryst. Growth* 311, 2063-2068 (2009).
- [20] Bertness, K. A., Sanders, A. W., Rourke, D. M., Harvey, T. E., Roshko, A., Schlager, J. B. and Sanford, N. A., "Controlled Nucleation of GaN Nanowires Grown with Molecular Beam Epitaxy," *Advanced Functional Materials* accepted, (2010).
- [21] Sekiguchi, H., Kishino, K. and Kikuchi, A., "Emission color control from blue to red with nanocolumn diameter of InGa_N/GaN nanocolumn arrays grown on same substrate," *Appl. Phys. Lett.* 96, 231104 (2010).
- [22] Hersee, S. D., Sun, X. Y. and Wang, X., "The controlled growth of GaN nanowires," *Nano Lett.* 6, 1808-1811 (2006).
- [23] Daudin, B., Widmann, F., Feuillet, G., Samson, Y., Arlery, M. and Rouvière, J. L., "Stranski-Krastanov growth mode during the molecular beam epitaxy of highly strained GaN," *Phys. Rev. B* 56, R7069 (1997).
- [24] Schlager, J. B., Bertness, K. A., Blanchard, P. T., Robins, L. H., Roshko, A. and Sanford, N. A., "Steady-state and time-resolved photoluminescence from relaxed and strained GaN nanowires grown by catalyst-free molecular-beam epitaxy," *J. Appl. Phys.* 103, 124309 (2008).
- [25] Schlager, J. B., Sanford, N. A., Bertness, K. A., Barker, J. M., Roshko, A. and Blanchard, P. T., "Polarization-resolved photoluminescence study of individual GaN nanowires grown by catalyst-free MBE," *Appl. Phys. Lett.* 88, 213106 (2006).
- [26] Meijers, R., Richter, T., Calarco, R., Stoica, T., Boehm, H. P., Marso, M. and Luth, H., "GaN-nanowhiskers: MBE-growth conditions and optical properties," *J. Cryst. Growth* 289, 381-386 (2006).
- [27] Chichibu, S. F., Yamaguchi, H., Zhao, L., Kubota, M., Okamoto, K. and Ohta, H., "Optical properties of nearly stacking-fault-free m-plane GaN homoepitaxial films grown by metal organic vapor phase epitaxy on low defect density freestanding GaN substrates," *Appl. Phys. Lett.* 92, 091912 (2008).
- [28] Schlager, J. B., Sanford, N. A., Bertness, K. A. and Roshko, A., "Injection-level-dependent internal quantum efficiency and lasing in low-defect GaN nanowires," submitted for publication, (2010).
- [29] Watanabe, S., Yamada, N., Nagashima, M., Ueki, Y., Sasaki, C., Yamada, Y., Taguchi, T., Tadatomo, K., Okagawa, H. and Kudo, H., "Internal quantum efficiency of highly-efficient In_xGa_{1-x}N-based near-ultraviolet light-emitting diodes," *Appl. Phys. Lett.* 83, 4906-4908 (2003).

- [30] Mansfield, L. M., Bertness, K. A., Blanchard, P. T., Harvey, T. E., Sanders, A. W. and Sanford, N. A., "GaN Nanowire Carrier Concentration Calculated from Light and Dark Resistance Measurements," *J. Electron. Mat.* 38, 495-504 (2009).
- [31] Sanford, N. A., Blanchard, P. T., Bertness, K. A., Mansfield, L., Schlager, J. B., Sanders, A. W., Roshko, A., Burton, B. B. and George, S. M., "Steady-state and transient photoconductivity in c-axis GaN nanowires grown by nitrogen-plasma-assisted molecular beam epitaxy," *J. Appl. Phys.* 107, 034318 (2010).
- [32] Calarco, R., Marso, M., Richter, T., Aykanat, A. I., Meijers, R., Hart, A. V., Stoica, T. and Luth, H., "Size-dependent photoconductivity in MBE-grown GaN-nanowires," *Nano Lett.* 5, 981-984 (2005).
- [33] Nikishin, S., Kipshidze, G., Kuryatkov, V., Choi, K., Gherasoiu, I., Grave de Peralta, L., Zubrilov, A., Tretyakov, V., Copeland, K., Prokofyeva, T., M. Holtz, M., Asomoza, R., Kudryavtsev, Y. and Temkin, H., "Gas source molecular beam epitaxy of high quality $\text{Al}_x\text{Ga}_{1-x}\text{N}$ ($0 \leq x \leq 1$) on Si(111)," *J. Vac. Sci. Technol. B* 19, 1409-1412 (2001).
- [34] Wunnicke, O., "Gate capacitance of back-gated nanowire field-effect transistors," *Appl. Phys. Lett.* 89, 083102 (2006).
- [35] Khanal, D. R. and Wu, J., "Gate coupling and charge distribution in nanowire field effect transistors," *Nano Lett.* 7, 2778-2783 (2007).
- [36] Blanchard, P. T., Bertness, K. A., Harvey, T. E., Mansfield, L. M., Sanders, A. W. and Sanford, N. A., "MESFETs Made From Individual GaN Nanowires," *IEEE Trans. Nanotechnol.* 7, 760-765 (2008).
- [37] Kikuchi, A., Kawai, M., Tada, M. and Kishino, K., "InGaN/GaN multiple quantum disk nanocolumn light-emitting diodes grown on (111)Si substrate," *Jpn. J. Appl. Phys. Part 2* 43, L1524-L1526 (2004).